

Species occurrence as a function of both emergent biological traits
and environmental context

Peter D. Smits^{1,*}

1. University of Chicago, Chicago, Illinois 60637.

* Corresponding author; e-mail: psmits@uchicago.edu.

Manuscript elements:

Keywords:

Manuscript type: Article

Prepared using the suggested L^AT_EX template for *Am. Nat.*

Introduction

- 2 How do species pools change over time as species are recruited or go extinct? When are ecotypes
enriched or depleted? How does global and regional environmental context affect the distribution of
4 species ecotypes (e.g. guilds) in a regional species pool?

A regional species pool is the set of species which form communities in a specific region; local
6 communities are subsets of the regional pool. The composition of a regional species pool changes
over time due to speciation, migration, extinction. Local scale processes like resource competition
8 only affect the regional species pool if all communities are affected.

Valentine and Bambach how they presented guilds in paleobiology which is taxa united by
10 similarity of their macroecology (Bambach, 1977; Valentine, 1969). Bush and Bambach presented
an ecocube to describe what how marine invertebrates partition space and resources (Bambach
12 et al., 2007; Bush and Bambach, 2011; Bush et al., 2007). Unique combinations represent what
possible ecotypes are observable. The distribution of ecocube occupancy is then normally analyzed
14 as raw counts of unique combinations or using ordination methods and the change in disparity over
time is estimated (Bambach et al., 2007; Bush and Bambach, 2011; Bush et al., 2007).

16 Analysis of mammal diversity and hypotheses as to the processes that have shaped it tend to fall
under a few categories: diversity of the whole system (Alroy, 1996; Alroy et al., 2000; Figueirido
18 et al., 2012; Liow et al., 2008), guild based (Janis et al., 2004, 2000; Janis and Wilhelm, 1993;
Jernvall and Fortelius, 2004; Pires et al., 2015), clade based (Quental and Marshall, 2013; Slater,
20 2015), climate based (Blois and Hadly, 2009; Janis, 1993; Janis and Wilhelm, 1993), and location
based (Badgley and Finarelli, 2013; Eronen et al., 2015). Rarely are more than two of these
22 categories considered simultaneously, and instead integration of these diverse observations and
hypotheses tends to be based on coincidence. The goal of this study is to pool information from
24 multiple levels of organization by integrating both species and climate data into a single analysis in
order to provide a more holistic interpretation of the processes which may have shaped mammal
26 species diversity.

Fourth-corner modeling is an approach to explaining the patterns of either species abundance or
28 presence/absence as a product of species traits, environmental factors, and the interaction between
traits and environment (Brown et al., 2014; Jamil et al., 2013; Pollock et al., 2012; Warton et al.,
30 2015) CITATION. In modern ecological studies, what is being modeled is species occurrences at
localities distributed across a region (Jamil et al., 2013; Pollock et al., 2012). In this study, what is
32 being modeled is the pattern of species occurrence over time for most of the Cenozoic in North
America (Fig. 1). These two approaches, modern and paleontological, are different views of the same
34 three-dimensional pattern: species at localities over time. The temporal limitations of modern
ecological studies and difficulties with uneven spatial occurrences of fossils in paleontological studies
36 means that these approaches are complimentary but reveal different patterns of how species are
distributed in time and space.

38 One of the greatest challenges with analyzing species occurrence data is the inherent incompleteness
of any sample (Foote, 2001; Foote and Sepkoski, 1999; Lloyd et al., 2011; Royle and Dorazio, 2008;
40 Royle et al., 2014; Wang and Marshall, 2016). In the modern, only presences are certain as an
absence can be caused by both the species being truly absent or the species never having been
42 sampled (Royle and Dorazio, 2008; Royle et al., 2014). For paleontological data in the context of
this study, the incomplete preservation of fossil communities combined with the incomplete
44 sampling of what fossils there are means that the true times of origination or extinction may not be
observed (Foote, 2001; Foote and Sepkoski, 1999; Wang et al., 2016; Wang and Marshall, 2016).

46 In the analyses done here, a few key covariates which describe species' macroecology and
environmental context are considered. Because of the complexity of fourth-corner analyses in terms
48 of both number of covariates considered and structure of each model, it is possible to consider and
test a large number of possible hypotheses. Presented here are the species traits and related
50 hypotheses, followed by the environmental factors and related hypotheses.

The principle species trait considered in this study is a species' ecotype, defined here as the unique
52 combination of species dietary category and locomotor category (e.g. arboreal omnivore versus
unguligrade herbivore). This classification is analogous to the marine invertebrate ecocube discussed

- 54 above (Bush and Bambach, 2011; Bush et al., 2007; ?). Species mass was also included as a species trait, but is mostly included in order to control for that effect on species observation and occurrence.
- 56 Translating previous work into hypotheses applicable to this analysis is difficult. Taxonomic grouping is frequently invoked in many proposed hypotheses for how mammal diversity is
- 58 structured (Janis and Wilhelm, 1993; Pires et al., 2015; Quental and Marshall, 2013; Slater, 2015). However, this practice is problematic because taxonomic grouping conflates shared evolutionary
- 60 history and similarities in species macroecology which means that whatever aspects of species biology are important for the processes underlying species diversity are obscured.
- 62 Many discussions of the effects or associates of species ecology and diversity have focused on ungulate herbivores (Janis et al., 2004, 2000; Janis and Wilhelm, 1993) CITATIONS JANIS 97
- 64 JANIS 08 and carnivores (Janis and Wilhelm, 1993; Pires et al., 2015; Slater, 2015) CITATIONS. Ungulate herbivores are characterized by younger originating taxa having longer legs, higher
- 66 crowned teeth, and a preference for grazing over browsing than earlier originating taxa (Janis et al., 2004, 2000; Janis and Wilhelm, 1993) CITATIONS JANIS 97 JANIS 08
- 68 Jernvall and Fortelius (2004) found that for the Neogene of Europe the relative abundance of mammal guilds was stable over time even in the face of high turnover rates.
- 70 Smits (2015) found several systematic differences in mammal species durations associated with various species traits. Omnivorous taxa were found to have, on average, a greater duration than
- 72 other dietary categories. Additionally, arboreal taxa were found to have a shorter duration than other locomotor categories.
- 74 An unresolved question from Smits (2015) is whether the greater extinction risk faced by arboreal is constant over time or if there was a change in extinction risk at the Paleogene/Neogene boundary.
- 76 Specifically, the question is whether the extinction risk arboreal taxa increased in the Neogene, driving the loss of arboreal taxa and average extinction risk of arboreal taxa down.
- 78 There are no observed massive cross-taxonomic turnover events in the North American record, unlike the Neogene record Europe (Alroy, 1996, 2009; Alroy et al., 2000; Eronen et al., 2015; Janis,

80 1993).

The environmental factors included in this study include estimates of global temperature and the
82 changing floral groups present in North America across the Cenozoic. Why are these factors
important? What are the hypotheses associated with environmental context?

84 Importantly, the probability of a species ecotype being present was modeled as a function of
environmental factors (Fig. 1).

86 The effect of climate on diversity and the diversification process has been the focus of considerable
research with many analyses favoring diversification being more biologically-mediated than
88 climate-mediated (Alroy, 1996; Alroy et al., 2000; Clyde and Gingerich, 1998; Figueirido et al.,
2012). Scale of analysis makes a big difference in interpretation of results, both temporal and
90 geographic. For example when the mammal fossil record analyzed at small temporal and geographic
scales a correlation between diversity and climate are observable (Clyde and Gingerich, 1998).

92 However, when the record is analyzed at the scale of the continent and the Cenozoic there is no
correlation with diversity and climate (Alroy et al., 2000). This result, however, does not go
94 against the idea that there may be short periods of correlation and that this correlation changes or
reverse direction over time; instead this result means that there is no single direction of correlation
96 between diversity and climate (Figueirido et al., 2012).

In the case of a fluctuating correlation between diversity and climate it is hard to make the
98 argument of an actual causal link between the two without understanding the ecological differences
in mammalian fauna over time; when this analysis is based on diversity or taxonomy alone no
100 mechanisms are possible to infer. After all, taxonomy conflates many potential factors that could
affect diversification into a single variable; by separating the effects of shared common ancestry (i.e.
102 phylogeny) from species ecology the subtle differences in the diversification process can be observed
(Smits, 2015).

104 There are many candidate climatic events that may have influenced the distribution of mammal
ecotypes regionally, if not globally (Blois and Hadly, 2009; Janis, 1993; Zachos et al., 2008, 2001).

106 The Paleocene-Eocene Thermal Maximum is associated with species dwarfing and rearrangement

of local communities, though regional effects are less known CITATION. The Mid-Miocene
108 climactic optimum is associated with WHAT CITATION. The

The general cooling throughout the Cenozoic and the development of ice-caps in the Neogene. The
110 Oligo-Miocene boundary.

One of the most stunning environmental transitions of the Cenozoic in North America was gradual
112 “opening-up” of the landscape with the shift from closed or partially forested environments of the
Paleogene to the savannah and grasslands environments that characterize the Neogene (Blois and
114 Hadly, 2009; Janis, 1993; Janis et al., 2000; Strömberg, 2005).

Ultimately, the goal of this analysis are to understand when are unique ecotypes enriched or
116 depleted in the North American mammal regional species pool and how changes in ecotypic
diversity are related to changes in species’ environmental context.

118 Materials and Methods

Taxon occurrences and species-level information

120 All fossil occurrence information information was downloaded from the Paleobiology Database.
Occurrences (PBDB) were restricted to all Mammalia sampled in North America between the
122 Maastrichtian and Gelasian stages. Taxonomic, stratigraphic, and ecological metadata for each
occurrence was included. The raw data is available for download at <http://goo.gl/2s1geU>.

124 This raw data was then sorted, cleaned, and manipulated programmatically prior to analysis.
Species taxonomic assignments given by the PBDB were updated for accuracy and consistency. For
126 example, species classified in the order Artiodactyla were reclassified as Cetartiodactyla. These
re-assignments follow Smits (2015) and were Janis et al. (2008, 1998) and the Encyclopedia of Life
128 WEBSITE. Additionally, Taxa who’s life habit was classified as either volant (i.e. Chiroptera) or
aquatic (e.g. Cetacea) were excluded from this analysis because of both differences in fossilization
130 potential and applicability to the study of terrestrial species pools.

The life habit and dietary categories provided through the PBDB were coarsened to increase per
 132 ecotype sample size; this coarsening follows the same procedure as Smits (2015). Additionally, life
 habit category was further modified to break-up the vague “ground-dwelling” category;
 134 re-classifying these species by ankle posture gives more precise information about that species’
 environmental context. Ground-dwelling taxa were reassigned following ? by species taxonomic
 136 context. Species ecotype is defined as the interaction between life habit and diet categories. Ecotype
 categories with less than 10 species having ever been in that combination were excluded, yielding a
 138 total of 18 of 24 possible ecotypes.

Table 1: Species trait assignments in this study are a coarser version of the information available in the PBDB. Information was coarsened to improve per category sample size and uniformity and followed this table.

This study		PBDB categories
Diet	Carnivore	Carnivore
	Herbivore	Browser, folivore, granivore, grazer, herbivore.
	Insectivore	Insectivore.
	Omnivore	Frugivore, omnivore.
Locomotor	Arboreal	Arboreal.
	Ground dwelling	Fossorial, ground dwelling, semifossorial, saltatorial.
	Scansorial	Scansorial.

Table 2: Posture assignment based on taxonomy

Order	Family	Stance
	Ailuridae	plantigrade
	Allomyidae	plantigrade
	Amphicyonidae	plantigrade
	Amphilemuridae	plantigrade
	Anthracotheriidae	digitigrade
	Antilocapridae	unguligrade
	Apheliscidae	plantigrade
	Aplodontidae	plantigrade
	Apternodontidae	scansorial

Continued on next page

Table 2 – continued from previous page

Order	Family	Stance
	Arctocyonidae	unguligrade
	Barbourofelidae	digitigrade
	Barylambdidae	plantigrade
	Bovidae	unguligrade
	Camelidae	unguligrade
	Canidae	digitigrade
	Cervidae	unguligrade
	Cimolodontidae	scansorial
	Coryphodontidae	plantigrade
	Cricetidae	plantigrade
	Cylindrodontidae	plantigrade
	Cyriacotheriidae	plantigrade
	Dichobunidae	unguligrade
Dinocerata		unguligrade
	Dipodidae	digitigrade
	Elephantidae	digitigrade
	Entelodontidae	unguligrade
	Eomyidae	plantigrade
	Erethizontidae	plantigrade
	Erinaceidae	plantigrade
	Esthonychidae	plantigrade
	Eutypomyidae	plantigrade
	Felidae	digitigrade
	Florentiamyidae	plantigrade
	Gelocidae	unguligrade

Continued on next page

Table 2 – continued from previous page

Order	Family	Stance
	Geolabididae	plantigrade
	Glyptodontidae	plantigrade
	Gomphotheriidae	unguligrade
	Hapalodectidae	plantigrade
	Heteromyidae	digitigrade
	Hyaenidae	digitigrade
	Hyaenodontidae	digitigrade
	Hypertragulidae	unguligrade
	Ischyromyidae	plantigrade
	Jimomyidae	plantigrade
Lagomorpha		digitigrade
	Leptictidae	plantigrade
	Leptochoeridae	unguligrade
	Leptomerycidae	unguligrade
	Mammutidae	unguligrade
	Megalonychidae	plantigrade
	Megatheriidae	plantigrade
	Mephitidae	plantigrade
	Merycoidodontidae	digitigrade
Mesonychia		unguligrade
	Mesonychidae	digitigrade
	Micropternodontidae	plantigrade
	Mixodectidae	plantigrade
	Moschidae	unguligrade
	Muridae	plantigrade

Continued on next page

Table 2 – continued from previous page

Order	Family	Stance
	Mustelidae	plantigrade
	Mylagaulidae	fossorial
	Mylodontidae	plantigrade
	Nimravidae	digitigrade
	Nothrotheriidae	plantigrade
Notoungulata		unguligrade
	Oromerycidae	unguligrade
	Oxyaenidae	digitigrade
	Palaeomerycidae	unguligrade
	Palaeoryctidae	plantigrade
	Pampatheriidae	plantigrade
	Pantolambdidae	plantigrade
	Peritychidae	digitigrade
Perissodactyla		unguligrade
	Phenacodontidae	unguligrade
Primates		plantigrade
	Procyonidae	plantigrade
	Proscalopidae	plantigrade
	Protoceratidae	unguligrade
	Reithroparamyidae	plantigrade
	Sciuravidae	plantigrade
	Sciuridae	plantigrade
	Simimyidae	plantigrade
	Soricidae	plantigrade
	Suidae	digitigrade

Continued on next page

Table 2 – continued from previous page

Order	Family	Stance
	Talpidae	fossorial
	Tayassuidae	unguligrade
	Tenrecidae	plantigrade
	Titanoideidae	plantigrade
	Ursidae	plantigrade
	Viverravidae	plantigrade
	Zapodidae	plantigrade

¹⁴⁰ Species mass information was gathered from multiple different sources where a plurality of the body size estimates are from the PBDB. Body part measurements for many species are also available
¹⁴² through the PBDB. Just as with Smits (2015), these measurements and corresponding regression equations were used to get mass estimates for more species. Additional mass estimates and body
¹⁴⁴ part measurements were sourced from numerous publications and the Neogene Old World Database; see the supplementary material to Smits (2015) for details. Mass was log-transformed and then
¹⁴⁶ mean-centered and rescaled by dividing by two-times its standard deviation; this insures that the magnitude of effects for both continuous and discrete covariates are comparable (Gelman, 2008;
¹⁴⁸ Gelman and Hill, 2007).

All fossil occurrences from 64 to 2 million years ago (Mya) were binned into 31 2 million year (My)
¹⁵⁰ bins. This temporal length was chosen because it is approximately the resolution of the North American mammal fossil record.

¹⁵² Environmental and temporal covariates

The group-level covariates in this study are descriptors of species' environmental context,
¹⁵⁴ specifically global temperature estimates and Graham's floral intervals CITATION. Global

Table 3: Regression equations used in this study for estimating body size. Equations are presented with reference to taxonomic grouping, part name, and reference.

Group	Equation	log(Measurement)	Source
General	$\log(m) = 1.827x + 1.81$	lower m1 area	Legendre (1986)
General	$\log(m) = 2.9677x - 5.6712$	mandible length	?
General	$\log(m) = 3.68x - 3.83$	skull length	?
Carnivores	$\log(m) = 2.97x + 1.681$	lower m1 length	?
Insectivores	$\log(m) = 1.628x + 1.726$	lower m1 area	?
Insectivores	$\log(m) = 1.714x + 0.886$	upper M1 area	?
Lagomorph	$\log(m) = 2.671x - 2.671$	lower toothrow area	Tomiya (2013)
Lagomorph	$\log(m) = 4.468x - 3.002$	lower m1 length	Tomiya (2013)
Marsupials	$\log(m) = 3.284x + 1.83$	upper M1 length	?
Marsupials	$\log(m) = 1.733x + 1.571$	upper M1 area	?
Rodentia	$\log(m) = 1.767x + 2.172$	lower m1 area	Legendre (1986)
Ungulates	$\log(m) = 1.516x + 3.757$	lower m1 area	?
Ungulates	$\log(m) = 3.076x + 2.366$	lower m2 length	?
Ungulates	$\log(m) = 1.518x + 2.792$	lower m2 area	?
Ungulates	$\log(m) = 3.113x - 1.374$	lower toothrow length	?

temperature across most of the Cenozoic was calculated from Mg/Ca isotope record from deep sea

156 carbonates (Cramer et al., 2011). Mg/Ca based temperature estimates are preferable to the
 frequently used $\delta^{18}\text{O}$ temperature proxy (Alroy et al., 2000; Figueirido et al., 2012; Zachos et al.,
 158 2008, 2001) because Mg/Ca estimates do not conflate temperature with ice sheet volume and
 depth/stratification changes; this makes it preferable as an estimate of global temperature for
 160 macroevolutionary and macroecological studies (Ezard et al., 2016).

Two aspects of the Mg/Ca-based temperature curve were included in this analysis: mean and range.

162 Both were calculated as the mean of all respective estimates for each 2 My temporal bins. Both
 mean and range were then rescaled as above: subtract mean, divide by twice the standard deviation.

164 The other major set of environmental factors included in this study are Graham's Cenozoic plant
 phases CITATION. Graham's plant phases are holistic descriptors of the taxonomic composition of
 166 which plants were present at a given time and their relative modernity, with younger phases
 representing increasingly modern taxa CITATION. Graham CITATION defines four intervals from
 168 the Cretaceous to the Pliocene, though only three of these intervals are included in this analysis.
 Graham's plant phases CITATION was included as a series of "dummy variables" encoding the

		State at $t + 1$		
		0_{never}	1	$0_{extinct}$
State at t	0_{never}	$1 - \theta$	θ	0
	1	0	θ	$1 - \theta$
	$0_{extinct}$	0	0	1

(a) Pure-presence

		State at $t + 1$		
		0_{never}	1	$0_{extinct}$
State at t	0_{never}	$1 - \phi$	ϕ	0
	1	0	π	$1 - \pi$
	$0_{extinct}$	0	0	1

(b) Birth-death

Table 4: Transition matrices for the pure-presence (4a) and birth-death (4b) models. Both of these models share the core machinery of discrete-time birth-death processes but make distinct assumptions about the equality of originating and surviving (Eq. 2, and 3). Note also that while there are only two state “codes” (0, 1), there are in fact three states: never having originated 0_{never} , present 1, extinct $0_{extinct}$ (Allen, 2011).

¹⁷⁰ three phases included in this analysis. This means that the first phase is synonymous with the intercept and phases

¹⁷² Modelling species occurrence

Two different models were used in this study: a pure-presence model and a birth-death model. Both ¹⁷⁴ models at their core are hidden Markov model where the latent aspect of the process has an absorbing state (Allen, 2011). The difference between these two models is if the probability of a ¹⁷⁶ species origination and survival are considered equal or different (Table 4). Something that is important to realize is that while there are only two state “codes” in a presence-absence matrix (i.e. ¹⁷⁸ 0/1), there are in fact three states in a birth-death model: never having originated, extant, and ¹⁸⁰ extinct. The last of these is the absorbing state, as once a species has gone extinct it cannot ¹⁸² re-originate (Allen, 2011); this is made obvious in the transition matrices as the probability of an extinct species changing states is 0 (Table 4). See below for parameter explanations (Tables 6, and 7).

Data augmentation

¹⁸⁴ All presence/absence observations are incomplete. The hidden Markov model at the core of this analysis allows for observed absences to be used meaningfully to estimate the number of unobserved ¹⁸⁶ species. Of specific concern in this analysis is the unknown “true” size of the dataset; how many

species could have actually been observed? While many species have been observed, the natural incompleteness of all observations, especially in the case of paleontological data, there are obviously many species which were never sampled (Royle and Dorazio, 2008; Royle et al., 2007).

Let N by the total number of observed species, M be the upper limit of possible species that could have existed given a model of species presence, and N^* is the all-zero histories where $N^* = M - N$. This approach assumes that $\hat{N} \sim \text{Binomial}(M, \psi)$ where \hat{N} is the estimated “true” number of species and ψ is the probability that any augmented species should actually be “present.” Because M is user defined, this approach effectively gives ψ a uniform prior over N to M (Royle and Dorazio, 2008). For this study, $M = N + \lfloor N/4 \rfloor$.

Data imputation is the process of estimating missing data for partially observed covariates (Gelman and Hill, 2007; Rubin, 1996), this is simple in a Bayesian context because data are also parameters (Gelman et al., 2013). Augmented species also have no known mass so a mass estimate must be imputed for each possible species (Royle and Dorazio, 2012). This procedure assumes that mass values for augmented species are from the same distribution as observed species. The distribution of observed mass values is estimated as part of the model, and new mass values are then generated from this distribution. This approach is an example of imputing data missing completely at random (Gelman and Hill, 2007; Royle and Dorazio, 2012). Because log mass values are rescaled as a part of this study, the body mass distribution is already known ($\mathcal{N}(0, 0.5)$); augmented species body mass just simply drawn from this distribution.

In addition to body mass information, the augmented species need an ecotype classification. Because these species are completely unknown, they were all classified as “augmented,” an additional grouping indicating their unknown biology. This classification has no biological interpretation.

Observation process

The type of hidden Markov model used in this study has three characteristic probabilities: probability p of observing a species given that it is present, probability ϕ of a species surviving from one time to another, and probability π of a species first appearing (Royle and Dorazio, 2008). In

Table 5: Observation parameters

Parameter	dimensions	explanation
y	$N \times T$	observed species presence/absence
z	$N \times T$	“true” species presence/absence
p	T	probability of observing a species that is present at time t
m	N	species log mass, rescaled
α_0	1	average log-odds of p
α_1	1	change in average log-odds of p per change mass
r	T	difference from α_0 associated with time t
σ	1	standard deviation of r

this formulation, the probability of a species going extinct is $1 - \pi$. For the pure-presence model

²¹⁴ $\phi = \pi$, while for the birth-death model $\phi \neq \pi$.

The probability of observing a species that is present p is modeled as a logistic regression was a
²¹⁶ time-varying intercept and species mass as a covariate. The effect of species mass on p was assumed
²¹⁸ linear and constant over time and given a prior reflecting a possible positive relationship; these
assumptions are reflected in the structure of the model Equation 1. The parameters associated with
this part of the model are described in Table 5.

$$\begin{aligned} y_{i,t} &\sim \text{Bernoulli}(p_{i,t} z_{i,t}) \\ p_{i,t} &= \text{logit}^{-1}(\alpha_0 + \alpha_1 m_i + r_t) \\ r_t &\sim \mathcal{N}(0, \sigma) \end{aligned} \tag{1}$$

²²⁰ **Pure-presence process**

For the pure-presence model there is only a single probability dealing with the presence of a species
²²² θ (Table 4a). This probability was modeled as multi-level logistic regression with both species-level
and group-level covariates (Gelman et al., 2013; Gelman and Hill, 2007). The parameters associated
²²⁴ with pure-presence model are presented in Table 6 and the full sampling statement in Equation 2.

The species-level of the model (Eq. 2) is a logistic regression with varying-intercept that varies by
²²⁶ ecotype. Additionally, species mass was included as a covariate associated with two regression

Table 6: Parameters for the model of presence in the pure-presence model

Parameter	dimensions	explanation
z	$N \times T$	“true” species presence/absence
θ	$N \times T - 1$	probability of $z = 1$
a	$T - 1 \times D$	ecotype-varying intercept; mean value of log-odds of θ
m	N	species log mass, rescaled
b_1	1	effect of species mass on log-odds of θ
b_2	1	effect of species mass, squared, on log-odds of θ
U	$T \times D$	matrix of group-level covariates
γ	$U \times D$	matrix of group-level regression coefficients
Σ	$D \times D$	covariance matrix of a
Ω	$D \times D$	correlation matrix of a
τ	D	vector of standard deviations for each ecotype a_d

coefficients allowing a quadratic relationship with log-odds of occurrence. This assumption is based

228 on the known distribution of mammal body masses where species with intermediate mass values are
 more common than either small or large bodied species. These assumptions are also reflected in the
 230 choice of priors for these regression coefficients.

The values of each ecotype’s intercept are themselves modeled as regressions using the group-level

232 covariates associated with environmental context. Each of these regressions has an associated
 variance of possible values of each ecotype’s intercept (Gelman and Hill, 2007). In addition, the
 234 covariances between ecotype intercepts, given this group-level regression, are modeled (Gelman and
 Hill, 2007).

236 All parameters not modeled elsewhere were given weakly informative priors (Gelman et al., 2013)
 CITATION STAN MANUAL STATISTICAL RETHINKING. Weakly informative means that
 238 priors do not necessarily encode actual prior information but instead help regularize or weakly
 constrain posterior estimates. These priors have a concentrated probability density around and near
 240 zero; this has the effect of tempering our estimates and help prevent overfitting the model to the

data (Gelman et al., 2013) CITATION STAN MANUAL STATISTICAL RETHINKING.

$$\begin{aligned}
y_{i,t} &\sim \text{Bernoulli}(p_{i,t} z_{i,t}) & \alpha_0 &\sim \mathcal{N}(0, 1) \\
p_{i,t} &= \text{logit}^{-1}(\alpha_0 + \alpha_1 m_i + r_t) & \alpha_1 &\sim \mathcal{N}(1, 1) \\
r_t &\sim \mathcal{N}(0, \sigma) & \sigma &\sim \mathcal{N}^+(1) \\
z_{i,1} &\sim \text{Bernoulli}(\rho) & b_1 &\sim \mathcal{N}(0, 1) \\
z_{i,t} &\sim \text{Bernoulli}(\theta_{i,t}) & b_2 &\sim \mathcal{N}(-1, 1) \\
\theta_{i,t} &= \text{logit}^{-1}(a_{t,j[i]} + b_1 m_i + b_2 m_i^2) & \gamma &\sim \mathcal{N}(0, 1) \\
a &\sim \text{MVN}(u\gamma, \Sigma) & \tau &\sim \mathcal{N}^+(1) \\
\Sigma &= \text{diag}(\tau)\Omega\text{diag}(\tau) & \Omega &\sim \text{LKJ}(2)
\end{aligned} \tag{2}$$

²⁴² Birth-death process

In the birth-death model, $\phi \neq \pi$ and so each of these probabilities are modeled separately but in a
²⁴⁴ similar manner to how θ is modeled in the pure-presence model (Eq. 2, Table 4b). The parameters
associated with the birth-death presence model are presented in Table 7 and the full sampling
²⁴⁶ statement, including observation (Eq. 1), is described in Equation 3.

Similar to the pure-presence model, both ϕ and π are modeled as logistic regressions with
²⁴⁸ varying-intercept and one covariate associated with two parameters. The possible relationships
between mass and both ϕ and π are reflected in the parameterization of the model and choice of
²⁵⁰ priors (Eq. 3).

The intercepts of ϕ and π both vary by species ecotype and those values are themselves the product
²⁵² of group-level regression using environmental factors as covariates (Eq. 3); this is identical to the

Table 7: Parameters for the model of presence in the pure-presence model

Parameter	dimensions	explanation
z	$N \times T$	“true” species presence/absence
ϕ	$N \times T$	probability of $z_{-,t} = 1 z_{-,t-1} = 0$
π	$N \times T - 1$	probability of $z_{-,t} = 1 z_{-,t-1} = 1$
a^ϕ	$T - 1 \times D$	ecotype-varying intercept; mean value of log-odds of θ
a^π	$T - 1 \times D$	ecotype-varying intercept; mean value of log-odds of θ
m	N	species log mass, rescaled
b_1^ϕ	1	effect of species mass on log-odds of ϕ
b_1^π	1	effect of species mass on log-odds of π
b_2^ϕ	1	effect of species mass, squared, on log-odds of ϕ
b_2^π	1	effect of species mass, squared, on log-odds of π
U	$T \times D$	matrix of group-level covariates
γ^ϕ	$U \times D$	matrix of group-level regression coefficients
γ^π	$U \times D$	matrix of group-level regression coefficients
Σ^ϕ	$D \times D$	covariance matrix of a^ϕ
Σ^π	$D \times D$	covariance matrix of a^π
Ω^ϕ	$D \times D$	correlation matrix of a^ϕ
Ω^π	$D \times D$	correlation matrix of a^π
τ^ϕ	D	vector of standard deviations for each ecotype a_d^ϕ
τ^π	D	vector of standard deviations for each ecotype a_d^π

pure presence model (Eq. 2).

$$\begin{aligned}
 y_{i,t} &\sim \text{Bernoulli}(p_{i,t} z_{i,t}) & \Sigma^\phi &= \text{diag}(\tau^\phi) \Omega^\phi \text{diag}(\tau^\phi) \\
 p_{i,t} &= \text{logit}^{-1}(\alpha_0 + \alpha_1 m_i + r_t) & \Sigma^\pi &= \text{diag}(\tau^\pi) \Omega^\pi \text{diag}(\tau^\pi) \\
 r_t &\sim \mathcal{N}(0, \sigma) & \rho &\sim U(0, 1) \\
 \alpha_0 &\sim \mathcal{N}(0, 1) & b_1^\phi &\sim \mathcal{N}(0, 1) \\
 \alpha_1 &\sim \mathcal{N}(1, 1) & b_1^\pi &\sim \mathcal{N}(0, 1) \\
 \sigma &\sim \mathcal{N}^+(1) & b_2^\phi &\sim \mathcal{N}(-1, 1) \\
 z_{i,1} &\sim \text{Bernoulli}(\phi_{i,1}) & b_2^\pi &\sim \mathcal{N}(-1, 1) \\
 z_{i,t} &\sim \text{Bernoulli} \left(z_{i,t-1} \pi_{i,t} + \sum_{x=1}^t (1 - z_{i,x}) \phi_{i,t} \right) & \gamma^\phi &\sim \mathcal{N}(0, 1) \\
 \phi_{i,t} &= \text{logit}^{-1}(a_{t,j[i]}^\phi + b_1^\phi m_i + b_2^\phi m_i^2) & \tau^\phi &\sim \mathcal{N}^+(1) \\
 \pi_{i,t} &= \text{logit}^{-1}(a_{t,j[i]}^\pi + b_1^\pi m_i + b_2^\pi m_i^2) & \tau^\pi &\sim \mathcal{N}^+(1) \\
 a^\phi &\sim \text{MVN}(U\gamma^\phi, \Sigma^\phi) & \Omega^\phi &\sim \text{LKJ}(2) \\
 a^\pi &\sim \text{MVN}(U\gamma^\pi, \Sigma^\pi) & \Omega^\pi &\sim \text{LKJ}(2)
 \end{aligned} \tag{3}$$

254 **Posterior inference and model adequacy**

Programs that implement joint posterior inference for the above models (Eqs. 2, 3) were
256 implemented in the probabilistic programming language Stan CITATION. The models used here
both feature latent discrete parameters in the large matrix z (Tables 5, 6, 7; Eqs. 1, 2, 3). All
258 methods for posterior inference implemented in Stan are derivative based which causes
complications for actually implementing the above models because integers do not have derivatives.
260 Instead of implementing a latent discrete parameterization, the posterior probabilities of all possible
states of the latent parameters z were estimated (i.e. marginalized).

262 Species durations at minimum range-through from the FAD to the LAD, but the incompleteness of
all observations means that the actual time of origination or extinction is unknown. The
264 marginalization approach used here means that the probabilities all possible histories for a species
are calculated, from the end members of the species having existed for the entire study interval and
266 the species having only existed between the directly observed FAD and LAD to all possible
intermediaries CITATION STAN MANUAL.

268 The combined size of the dataset and large number of parameters in both models (Eqs. 2, 3),
specifically the total number of latent parameters that are the matrix z , means that stochastic
270 approximate posterior inference is computationally very slow even using HMC. Instead, an
approximate Bayesian approach was used: variational inference. A recently developed automatic
272 variational inference algorithm called “automatic differentiation variational inference” (ADVI) is
implemented in Stan and was used here CITATION. ADVI assumes that the posterior is Gaussian
274 but still yields a true Bayesian posterior; this assumption is similar to quadratic approximation of
the likelihood function used in maximum likelihood inference CITATION. The principal limitation
276 of assuming the joint posterior is Gaussian is that the true topology of the log-posterior isn’t
estimated; this is a particular burden for scale parameters which are bound to be positive (e.g.
278 standard deviation).

After fitting both models (Eqs. 2, 3) using ADVI, model adequacy and quality of fit was assessed
280 using a series of posterior predictive checks CITATION CITATION. Because all Bayesian models

- are inherently generative, simulations of new data sets is “free” CITATION. By simulating many
 282 theoretical data sets using the observed covariate information the congruence between predictions
 made by the model and the observed empirical data can be assessed. By combining multiple
 284 posterior predictive tests of congruence between empirical and simulated values of interest, the
 holistic adequacy of the model can be analyzed CITATION.
- 286 An example posterior predictive check used in this study was comparing the observed average
 number of observations per species to a distribution of simulated averages; if the empirically
 288 observed value sits in the middle of the distribution than the model is adequate in reproducing the
 observed number of occurrences per species.
- 290 Posterior simulations for time series are start with the values at $t = 1$ and then just simulating
 forward.
- 292 Given parameter estimates, diversity and diversification rates are estimated through posterior
 predictive simulations. Given the observed presence-absence matrix y , estimates of the true
 294 presence-absence matrix z can be simulated and the distribution of possible occurrence histories
 can be analyzed. This is conceptually similar to marginalization where the probability of each
 296 possible occurrence history is estimated (Fig. 2).

The posterior distribution of z gives the estimate of standing diversity N_t^{stand} for all time points as

$$N_t^{stand} = \sum_{i=1}^M z_{i,t}. \quad (4)$$

- 298 Given estimates of N^{stand} for all time points, the estimated number of originations O_t are be
 estimated as

$$O_t = \sum_{i=1}^M z_{i,t} = 1 | z_{i,t-1} = 0 \quad (5)$$

- 300 and number of extinctions E_t estimated as

$$E_t = \sum_{i=1}^M z_{i,t} = 0 | z_{i,t-1} = 1. \quad (6)$$

Per-capita growth D^{rate} , origination O^{rate} and extinction E^{rate} rates are then calculated as

$$\begin{aligned} O_t^{rate} &= \frac{O_t}{N_{t-1}^{stand}} \\ E_t^{rate} &= \frac{E_t}{N_{t-1}^{stand}} \\ D_t^{rate} &= O_t^{rate} - E_t^{rate}. \end{aligned} \tag{7}$$

302 Results

Posterior results take one of two forms: direct inspection of parameter estimates, and downstream
304 estimates of diversity and diversification rates. For the former, both the pure-presence and
birth-death models (Eq. 2, and 3 are inspected. For the latter, only posterior estimates from the
306 birth-death model are considered; the reason for this is explained below in the comparison of the
models' posterior predictive check results.

308 Comparing parameter estimates from the pure-presence and birth-death models

310 Comparison of the posterior predictive performance of the pure-presence and birth-death models
reveals a striking difference in quality of the models' fits to the data (Fig. 3a and 3b). The
312 birth-death model is clearly able to reproduce the observed average number of occurrence, in
contrast to the pure-birth model which greatly underestimates the ovserved average number of
314 occurrences. The interpretation of these results is that the results of the birth-death model are
more representative of the data than the pure-presence model, though further inspection of the
316 posterior parameter estimates can provide further insight into why these models give different
posterior predictive results (Gelman et al., 2013). However, it is expected that downstream analyses
318 from the birth-death model will be more reliable than that from the pure-presence model.

Occurrence probabilities estimated from the pure-presence model (Fig. 4) are much more similar to
320 the origination estimates from the birth-death model (Fig. 5) than the estimates of survival

probability (Fig. 6).

- 322 In general, both occurrence probabilities estimated from the pure-presence model (Fig. 4) and
origination probabilities estimated from the birth-death model (fig. 5) increase with time. Notable,
324 ecotypes with arboreal components do not follow this average; instead, occurrence and origination
probabilities appear relatively flat for most of the Cenozoic.
- 326 The dramatic differences between origination and survival probabilities indicate how different these
processes are, and may be responsible for the better posterior predictive performance of the
328 birth-death model over the pure-presence model (Fig. 3a, and 3b). While the estimates of both time
series have high variance, what is striking is how mean origination probability changes over time
330 while in general survival probabilities have relatively stable means (Fig. 5, and 6).

Estimates of origination probabilities appear to have less uncertainty than for survival (Fig. 5, and
332 6).

The pure-presence and birth-death models differ in estimated effect of mass on the probability of
334 observing a species that is present (Fig. 7). For the pure-presence model, mass is estimated to have
no effect on the probability of observing a species that is present (Fig. 7a). Contrastingly, for the
336 birth-death model mass is found to have a negative relationship with observation such that larger
species are less likely to be observed if present than smaller species (Fig. 7b).

- 338 The result from the birth-death model is unexpected given that it is generally assumed that larger
mammals are more likely to have been collected than smaller mammals CITATION. However,
340 collection is not preservation; similarities in preservation rate indicate similarities in how gap-filled
species records are. What this result means is that the record of large bodied species is expected on
342 average to be more gap-filled and less consistent from time point to time point than smaller bodied
species. Additionally, this is presence/absence data, so higher preservation and collection in terms
344 of individual specimens at a location or a single temporal horizon does not necessarily translate to
high preservation over time.
- 346 The effect of species mass on probability of occurrence as estimated from the pure-presence (Fig. 8)

is most similar to the effect of species mass on probability of origination as estimates from the
348 birth-death model (Fig. 9). The striking pattern observable in both sets of estimates is the higher
probability of occurrence for species with body sizes closer to the mean than either extremes. This
350 result is consistent with the canonically normal distribution of mammal body sizes CITATION; it is
then expected that the most likely to occur species would be those from the middle of the
352 distribution, and that species originating will on average be of average mass, especially considering
species shared common ancestry CITATION.

354 In contrast, the effect of species mass on probability of survival as estimated from the birth-death
model (Fig. 10) indicates little effect of mass on extinction; this is consistent with previous findings
356 from the North American mammal fossil record (Smits, 2015; Tomiya, 2013). Note that all variation
between ecotypes is due to differences in ecotype-specific survival probability and the associated
358 effects of plant phase.

Similarities in parameters estimates between ecotypes may be due to similar response to
360 environmental factors. Some of the obvious patterns from inspection of the individual-level
estimates of occurrence (Fig. 4), origination (Fig. 5), and survival probabilities (Fig. 6) that are of
362 note are the similarities between arboreal taxa and the differences between arboreal and all other
taxa.

364 Inspection of parameter estimates for the group-level covariates

Analysis of diversity

366 All analyses of diversification and macroevolutionary rates has been done using only the birth-death
model; this is because of the models better posterior predictive check performance (Fig. 3a, and 3b).
368 For the first half of the Cenozoic there appears to be a very slow decline and then plateau in total
diversity until the WHEN? (Fig. 14a).
370 When viewed through the lens of diversification rate the structure behind this pattern begins to
take shape (Fig. 14b). For approximately the first third of the Cenozoic, diversification rate is

³⁷² frequently below zero species gained per species present per two million years; this is broken up by few inferred spikes in diversification WHEN?. During the observed period of possible stability in

³⁷⁴ The comparison between per capita origination and extinction rate estimates reveals how diversification rate is formed (Fig. 14c, 14d). Origination rate seems most closely mimic
³⁷⁶ diversification rate while extinction rate has a saw-toothed pattern for the Cenozoic with no obvious emergent structure; inferred spikes in origination rate do not correspond to any spikes in
³⁷⁸ extinction rate.

Diversity partitioned by ecotype reveals a lot of the complexity behind the pattern of mammal
³⁸⁰ diversity for the Cenozoic (Fig. 15).

An impressive commonality across multiple ecotype-specific diversity time series are two spikes in
³⁸² diversity, either up or down (Fig. 15). Spikes of increased diversity are seen this is seen in all arboreal ecotypes, plantigrade insectivores, scansorial insectivores, and scansorial omnivores. The
³⁸⁴ converse pattern, spikes of decreased diversity, are strongly observed in the diversity history of digitigrade herbivores, with weaker decreases observed in the histories of digitigrade carnivores, and
³⁸⁶ unguligrade herbivores.

Arboreal ecotypes are estimated to have disappeared and reappeared as short bursts over the last
³⁸⁸ 65 million years in North America, with arboreal carnivores and insectivores being most often rarer than arboreal herbivores and omnivores.

³⁹⁰ Fossorial ecotypes, whether herbivorous and insectivorous appear rare or possibly absent for most the Cenozoic, which maximum estimated diversity being obtained in the latter half of the time
³⁹² series (Fig. 15).

Plantigrade ecotypes appear most variable, plantigrade herbivores having a very different diversity history than plantigrade carnivores and omnivores and plantigrade insectivores.

Unguligrade and plantigrade herbivores have relatively stable standing diversities throughout the
³⁹⁶ Cenozoic of North America (Fig. 15). Similarly, digitigrade carnivorous taxa appear to have a relatively stable diversity for the Cenozoic.

³⁹⁸ **Discussion**

Acknowledgements

⁴⁰⁰ I would like to thank K. Angielczyk, M. Foote, P. D. Polly, and R. Ree for helpful discussion and advice. This entire study would not have been possible without the Herculean effort of the
⁴⁰² many contributors to the Paleobiology Database. In particular, I would like to thank J. Alroy and M. Uhen for curating most of the mammal occurrences recorded in the PBDB. This is Paleobiology
⁴⁰⁴ Database publication XXX.

References

- ⁴⁰⁶ Allen, L. J. S. 2011. An introduction to stochastic processes with applications to biology. 2nd ed. Chapman and Hall/CRC, Boca Raton, FL.
- ⁴⁰⁸ Alroy, J. 1996. Constant extinction, constrained diversification, and uncoordinated stasis in North American mammals. *Palaeogeography, Palaeoclimatology, Palaeoecology* 127:285–311.
- ⁴¹⁰ ———. 2009. Speciation and extinction in the fossil record of North American mammals. Pages 302–323 *in* R. K. Butlin, J. R. Bridle, and D. Schlüter, eds. *Speciation and patterns of diversity*.
⁴¹² Cambridge University Press, Cambridge.
- Alroy, J., P. L. Koch, and J. C. Zachos. 2000. Global climate change and North American
⁴¹⁴ mammalian evolution. *Paleobiology* 26:259–288.
- Badgley, C., and J. A. Finarelli. 2013. Diversity dynamics of mammals in relation to tectonic and
⁴¹⁶ climatic history: comparison of three Neogene records from North America. *Paleobiology*
39:373–399.
- ⁴¹⁸ Bambach, R. K. 1977. Species richness in marine benthic habitats through the Phanerozoic.
Paleobiology 3:152–167.

- ⁴²⁰ Bambach, R. K., A. M. Bush, and D. H. Erwin. 2007. Autecology and the filling of ecospace: Key metazoan radiations. *Palaeontology* 50:1–22.
- ⁴²² Blois, J. L., and E. A. Hadly. 2009. Mammalian Response to Cenozoic Climatic Change. *Annual Review of Earth and Planetary Sciences* 37:181–208.
- ⁴²⁴ Brown, A. M., D. I. Warton, N. R. Andrew, M. Binns, G. Cassis, and H. Gibb. 2014. The fourth-corner solution - using predictive models to understand how species traits interact with
⁴²⁶ the environment. *Methods in Ecology and Evolution* 5:344–352.
- Bush, A. M., and R. K. Bambach. 2011. Paleoeologic Megatrends in Marine Metazoa, vol. 39.
- ⁴²⁸ Bush, A. M., R. K. Bambach, and G. M. Daley. 2007. Changes in theoretical ecospace utilization in marine fossil assemblages between the mid-Paleozoic and late Cenozoic. *Paleobiology* 33:76–97.
- ⁴³⁰ Clyde, W. C., and P. D. Gingerich. 1998. Mammalian community response to the latest Paleocene thermal maximum: an isotaphonomic study in the northern Bighorn Basin, Wyoming. *Geology*
⁴³² 26:1011–1014.
- Cramer, B. S., K. Miller, P. Barrett, and J. Wright. 2011. Late Cretaceous-Neogene trends in deep
⁴³⁴ ocean temperature and continental ice volume: Reconciling records of benthic foraminiferal geochemistry ($\delta^{18}\text{O}$ and Mg/Ca) with sea level history. *Journal of Geophysical Research: Oceans*
⁴³⁶ 116:1–23.
- Eronen, J. T., C. M. Janis, C. P. Chamberlain, and A. Mulch. 2015. Mountain uplift explains
⁴³⁸ differences in Palaeogene patterns of mammalian evolution and extinction between North America and Europe. *Proceedings of the Royal Society B: Biological Sciences* 282:20150136.
- ⁴⁴⁰ Ezard, T. H. G., A. Purvis, and H. Morlon. 2016. Environmental changes define ecological limits to species richness and reveal the mode of macroevolutionary competition. *Ecology Letters*
⁴⁴² 19:899–906.
- Figueirido, B., C. M. Janis, J. A. Pérez-Claros, M. De Renzi, and P. Palmqvist. 2012. Cenozoic

- 444 climate change influences mammalian evolutionary dynamics. *Proceedings of the National
Academy of Sciences* 109:722–727.
- 446 Foote, M. 2001. Inferring temporal patterns of preservation, origination, and extinction from
taxonomic survivorship analysis. *Paleobiology* 27:602–630.
- 448 Foote, M., and J. J. Sepkoski. 1999. Absolute measures of the completeness of the fossil record.
Nature 398:415–7.
- 450 Gelman, A. 2008. Scaling regression inputs by dividing by two standard deviations. *Statistics in
Medicine* pages 2865–2873.
- 452 Gelman, A., J. B. Carlin, H. S. Stern, D. B. Dunson, A. Vehtari, and D. B. Rubin. 2013. Bayesian
data analysis. 3rd ed. Chapman and Hall, Boca Raton, FL.
- 454 Gelman, A., and J. Hill. 2007. Data Analysis using Regression and Multilevel/Hierarchical Models.
Cambridge University Press, New York, NY.
- 456 Jamil, T., W. A. Ozinga, M. Kleyer, and C. J. F. Ter Braak. 2013. Selecting traits that explain
species-environment relationships: A generalized linear mixed model approach. *Journal of
Vegetation Science* 24:988–1000.
- Janis, C., J. Damuth, and J. M. Theodor. 2004. The species richness of Miocene browsers, and
460 implications for habitat type and primary productivity in the North American grassland biome.
Palaeogeography, Palaeoclimatology, Palaeoecology 207:371–398.
- 462 Janis, C. M. 1993. Tertiary mammal evolution in the context of changing climates, vegetation, and
tectonic events. *Annual Review of Ecology and Systematics* 24:467–500.
- 464 Janis, C. M., J. Damuth, and J. M. Theodor. 2000. Miocene ungulates and terrestrial primary
productivity: where have all the browsers gone? *Proceedings of the National Academy of Sciences*
466 97:7899–904.
- Janis, C. M., G. F. Gunnell, and M. D. Uhen. 2008. Evolution of Tertiary mammals of North

- 468 America. Vol. 2. Small mammals, xenarthrans, and marine mammals. Cambridge University
Press, Cambridge.
- 470 Janis, C. M., K. M. Scott, and L. L. Jacobs. 1998. Evolution of Tertiary mammals of North
America. Vol. 1. Terrestrial carnivores, ungulates, and ungulatelike mammals. Cambridge
472 University Press, Cambridge.
- Janis, C. M., and P. B. Wilhelm. 1993. Were there mammalian pursuit predators in the tertiary?
474 Dances with wolf avatars. *Journal of Mammalian Evolution* 1:103–125.
- Jernvall, J., and M. Fortelius. 2004. Maintenance of trophic structure in fossil mammal
476 communities: site occupancy and taxon resilience. *The American Naturalist* 164:614–624.
- Legendre, S. 1986. Analysis of mammalian communities from the Late Eocene and Oligocene of
478 Southern France. *Paleovertebrata* 16:191–212.
- Liow, L. H., M. Fortelius, E. Bingham, K. Lintulaakso, H. Mannila, L. Flynn, and N. C. Stenseth.
480 2008. Higher origination and extinction rates in larger mammals. *Proceedings of the National
Academy of Sciences* 105:6097–6102.
- 482 Lloyd, G. T., J. R. Young, and A. B. Smith. 2011. Taxonomic Structure of the Fossil Record is
Shaped by Sampling Bias. *Systematic Biology* 61:80–89.
- 484 Pires, M. M., D. Silvestro, and T. B. Quental. 2015. Continental faunal exchange and the
asymmetrical radiation of carnivores. *Proceedings of the Royal Society B: Biological Sciences*
486 282:20151952.
- Pollock, L. J., W. K. Morris, and P. A. Vesk. 2012. The role of functional traits in species
488 distributions revealed through a hierarchical model. *Ecography* 35:716–725.
- Quental, T. B., and C. R. Marshall. 2013. How the Red Queen Drives Terrestrial Mammals to
490 Extinction. *Science* 341:290–292.
- Royle, J. A., and R. M. Dorazio. 2008. Hierarchical modeling and inference in ecology: the analysis
492 of data from populations, metapopulations and communities. Elsevier, London.

- . 2012. Parameter-expanded data augmentation for Bayesian analysis of capture-recapture models. *Journal of Ornithology* 152:521–537.
- 494
- Royle, J. A., R. M. Dorazio, and W. a. Link. 2007. Analysis of Multinomial Models With Unknown Index Using Data Augmentation. *Journal of Computational and Graphical Statistics* 16:67–85.
- 496
- Royle, J. A., J. D. Nichols, M. Kéry, E. Ranta, and M. Kery. 2014. detection is of species when Modelling occurrence and abundance imperfect 110:353–359.
- 498
- Rubin, D. B. 1996. Multiple imputation after 18+ years. *Journal of the American Statistical Association* 91:473–489.
- 500
- Slater, G. J. 2015. Iterative adaptive radiations of fossil canids show no evidence for diversity-dependent trait evolution. *Proceedings of the National Academy of Sciences* 112:4897–4902.
- 502
- 504 Smits, P. D. 2015. Expected time-invariant effects of biological traits on mammal species duration. *Proceedings of the National Academy of Sciences* 112:13015–13020.
- 506 Strömberg, C. A. E. 2005. Decoupled taxonomic radiation and ecological expansion of open-habitat grasses in the Cenozoic of North America. *Proceedings of the National Academy of Sciences of the United States of America* 102:11980–4.
- 508
- Tomiya, S. 2013. Body Size and Extinction Risk in Terrestrial Mammals Above the Species Level. *The American Naturalist* 182:196–214.
- 510
- Valentine, J. W. 1969. Patterns of taxonomic and ecological structure of the shelf benthos during Phanerozoic time. *Paleontology* 12:684–709.
- 512
- 514 Wang, S. C., P. J. Everson, H. J. Zhou, D. Park, and D. J. Chudzicki. 2016. Adaptive credible intervals on stratigraphic ranges when recovery potential is unknown. *Paleobiology* 42:240–256.
- Wang, S. C., and C. R. Marshall. 2016. Estimating times of extinction in the fossil record. *Biology Letters* 12:20150989.
- 516

- Warton, D. I., B. Shipley, and T. Hastie. 2015. CATS regression - a model-based approach to
518 studying trait-based community assembly. *Methods in Ecology and Evolution* 6:389–398.
- Zachos, J. C., G. R. Dickens, and R. E. Zeebe. 2008. An early Cenozoic perspective on greenhouse
520 warming and carbon-cycle dynamics. *Nature* 451:279–283.
- Zachos, J. C., M. Pagani, L. Sloan, E. Thomas, and K. Billups. 2001. Trends, rhythms, and
522 aberrations in global climate 65 Ma to present. *Science* 292:686–693.

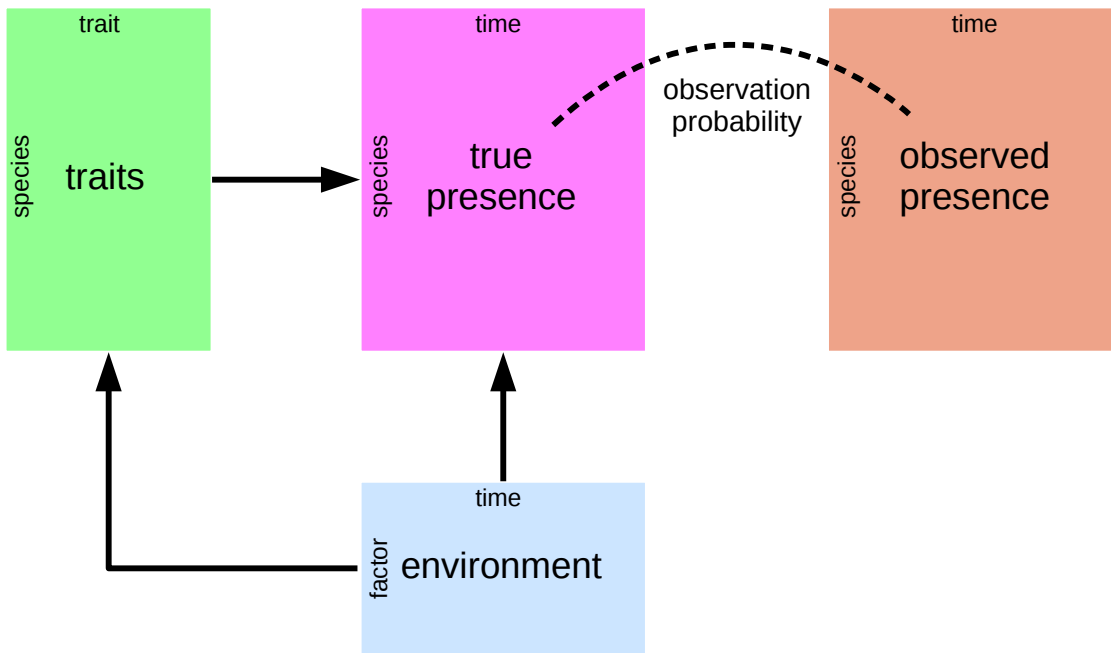


Figure 1: Conceptual diagram of the paleontological fourth corner problem. The observed presence matrix (orange) is the empirical presence/absence pattern for all species for all time points; this matrix is an incomplete observation of the “true” presence/absence pattern (purple). The estimated true presence matrix is modeled as a function of both environmental factors over time (blue) and multiple species traits (green). Additionally, the effect of environmental factors on species traits are also modeled as traits are expected to mediate the effects of a species environmental context. This diagram is based partially on material presented in Brown et al. (2014) and Warton et al. (2015).

	Time Bin							
	1	2	3	4	5	6	7	8
Observed	0	0	0	1	0	1	1	0
Certain	?	?	?	1	1	1	1	?
Potential	0	0	0	1	1	1	1	0
Potential	0	0	1	1	1	1	1	0
Potential	0	1	1	1	1	1	1	0
Potential	1	1	1	1	1	1	1	0
Potential	0	0	0	1	1	1	1	1
Potential	0	0	1	1	1	1	1	1
Potential	0	1	1	1	1	1	1	1
Potential	1	1	1	1	1	1	1	1

Figure 2: Conceptual figure of all possible occurrence histories for an observed species. The first row represents the observed presence/absence pattern for a single species at eight time points. The second row corresponds to the known aspects of the “true” occurrence history of that species. The remaining rows correspond to all possible occurrence histories that are consistent with the observed data. The process of parameter marginalization described in the text

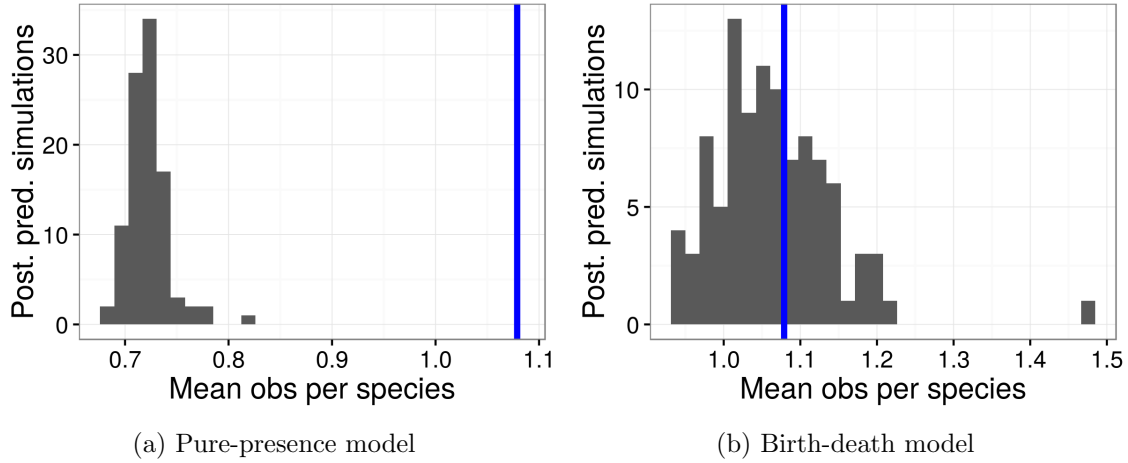


Figure 3: Comparison of the average observed number of occurrences per species (blue line) to the average number of occurrences from 100 posterior predictive datasets using the posterior estimates from the pure-presence and birth-death models.

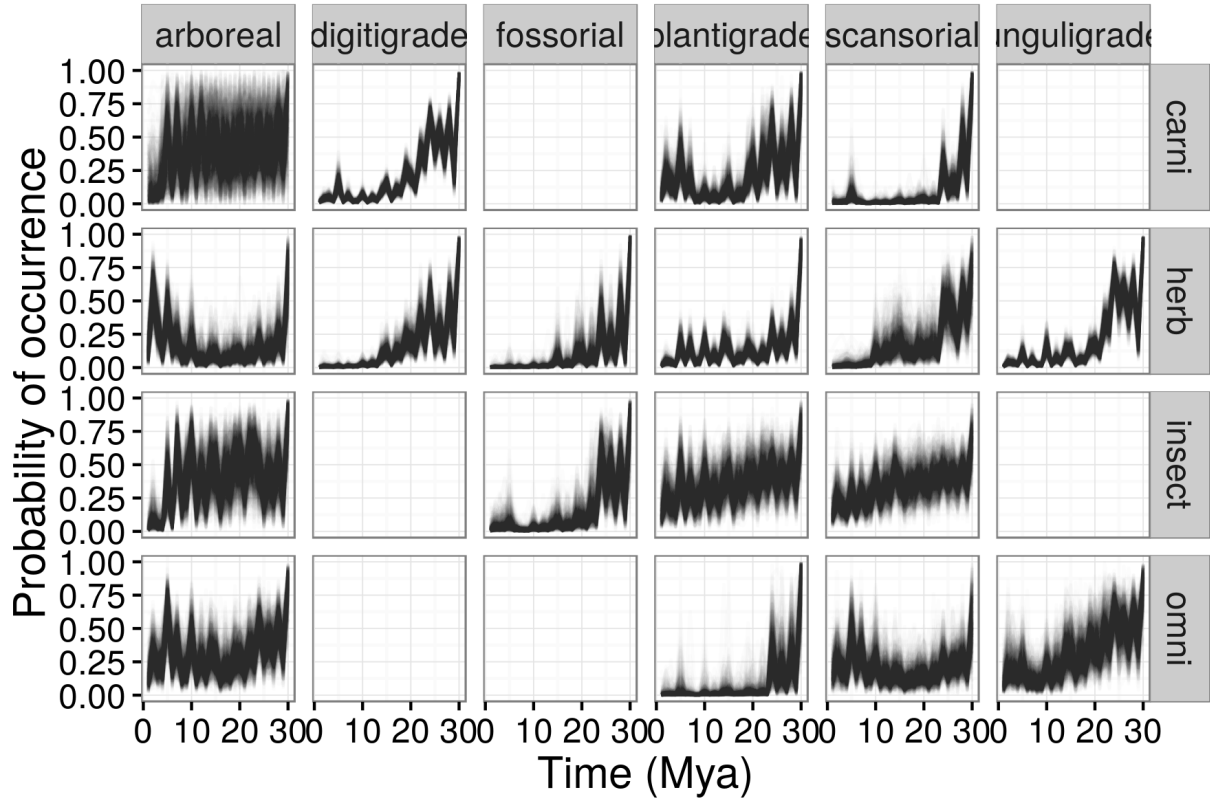


Figure 4: Probability of a mammal ecotype occurring over time as estimated from the pure-presence model. Each panel depicts 100 random samples from the model's posterior. The columns are by locomotor category and rows by dietary category; their intersections are the observed and analyzed ecotypes. Panels with no lines are ecotypes not observed in the dataset.

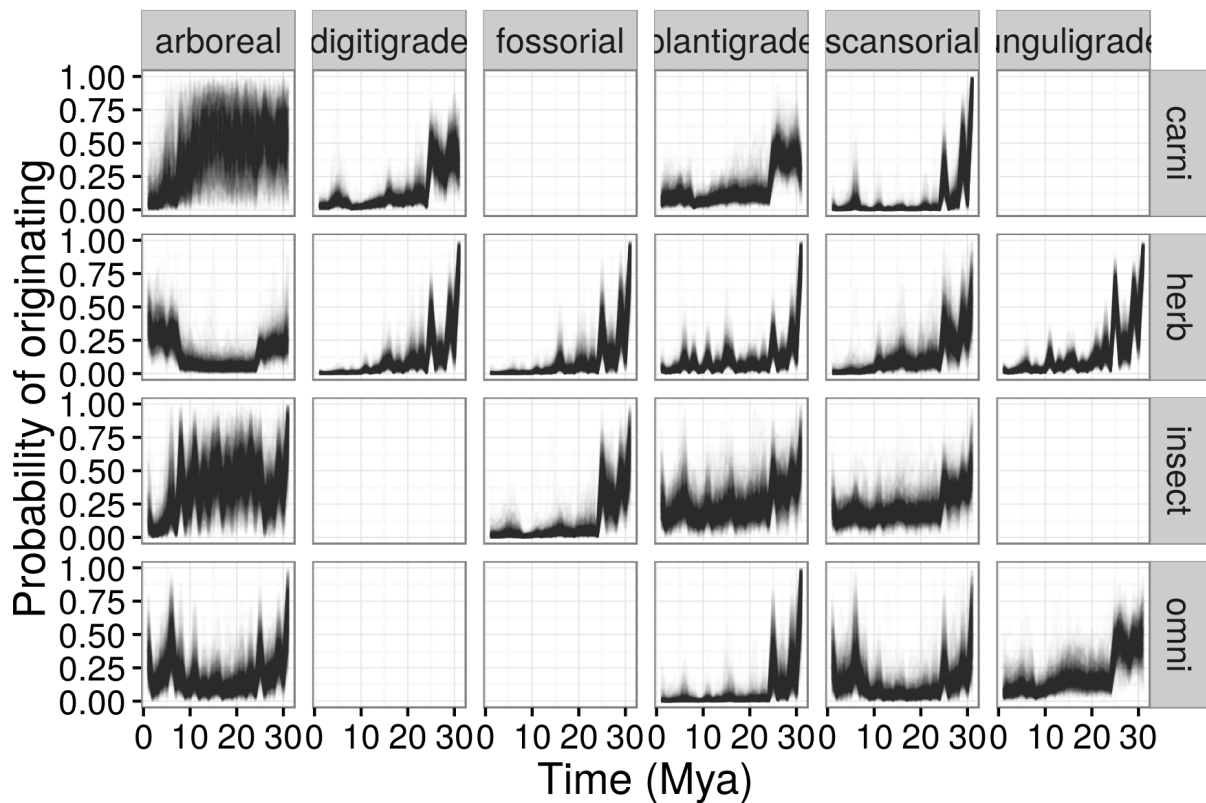


Figure 5: Probability of a mammal ecotype origination probabilities at each time point as estimated from the birth-death model. Each panel depicts 100 random samples from the model's posterior. The columns are by locomotor category and rows by dietary category; their intersections are the observed and analyzed ecotypes. Panels with no lines are ecotypes not observed in the dataset.

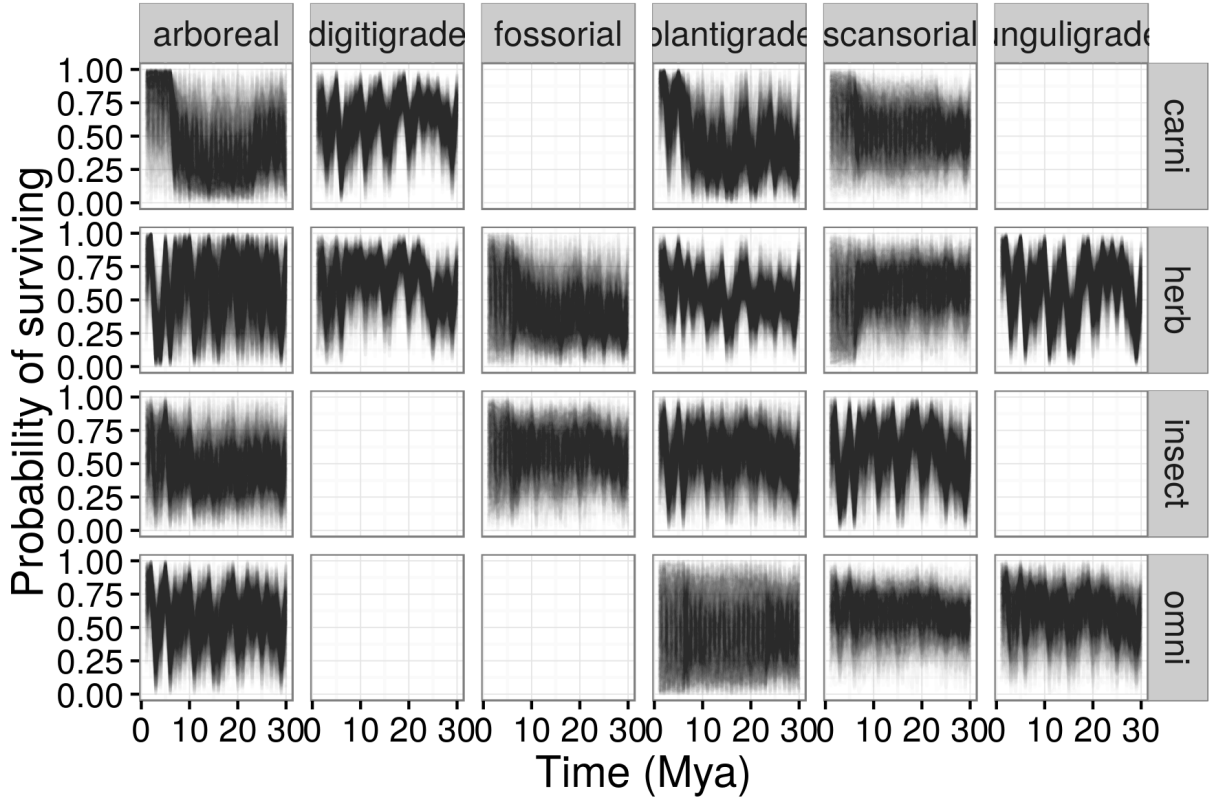


Figure 6: Probability of a mammal ecotype survival probabilities at each time point as estimated from the birth-death model. Each panel depicts 100 random samples from the model’s posterior. The columns are by locomotor category and rows by dietary category; their intersections are the observed and analyzed ecotypes. Panels with no lines are ecotypes not observed in the dataset.

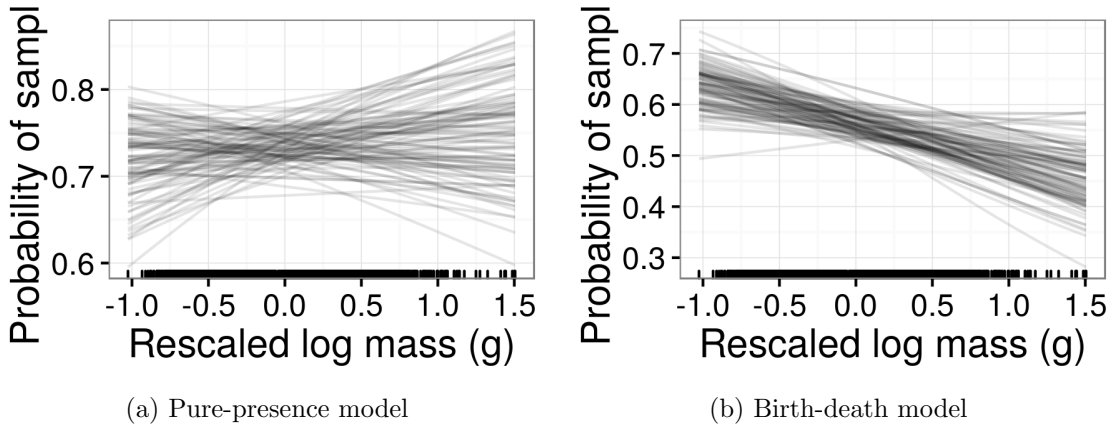


Figure 7: Estimates of the effect of species mass on probability of observing a present species (p). Mass has been log-transformed, centered, and rescaled; this means that a mass of 0 corresponds to the mean of log-mass of all observed species and that mass is in standard deviation units. Estimates are from both the pure-presence and birth-death models.

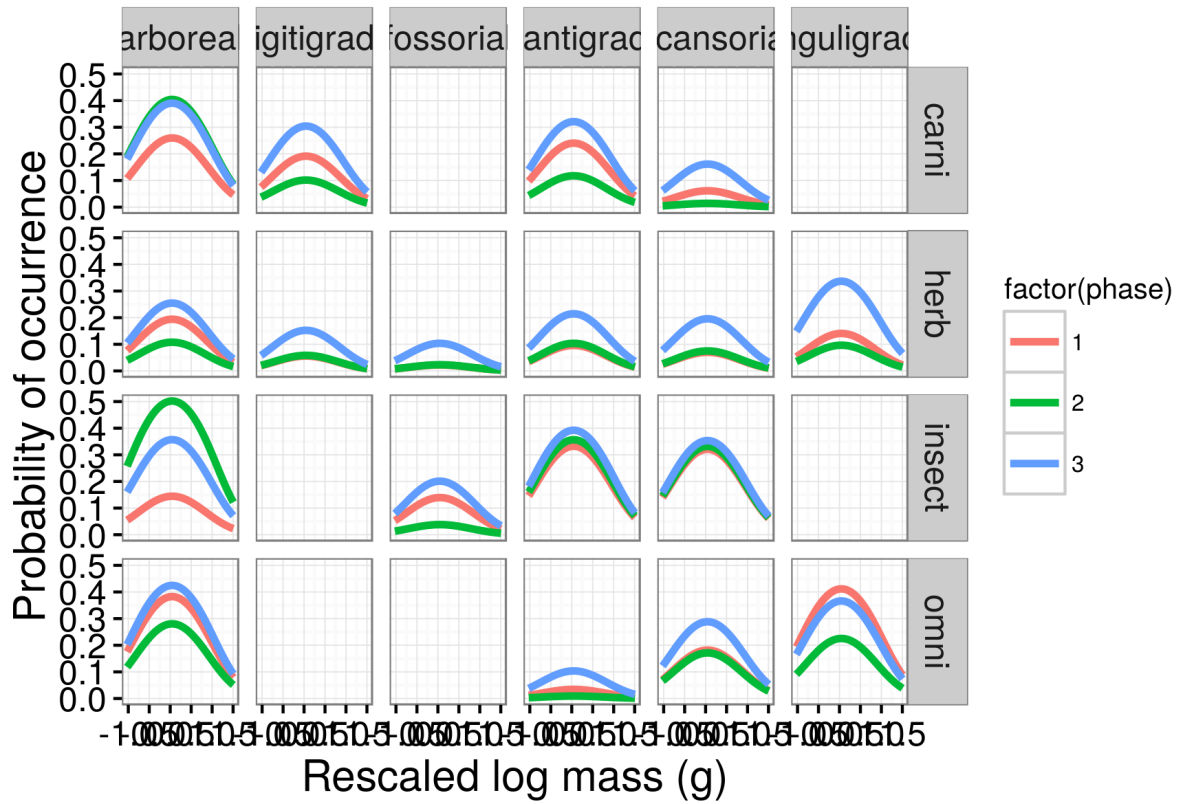


Figure 8: Mean estimate of the effect of species mass on the probability of a species occurrence for each of the three plant phases. The effect of mass is considered constant over time and that the only aspect of the model that changes with plant phase is the intercept of the relationship between mass and occurrence. The three plant phases are indicated by the color of the line. Mass has been log-transformed, centered, and rescaled; this means that a mass of 0 corresponds to the mean of log-mass of all observed species and that mass is in standard deviation units. Only the mean estimates of the effects of both mass and plant phase are plotted for clarity; these estimates are obviously made with uncertainty.

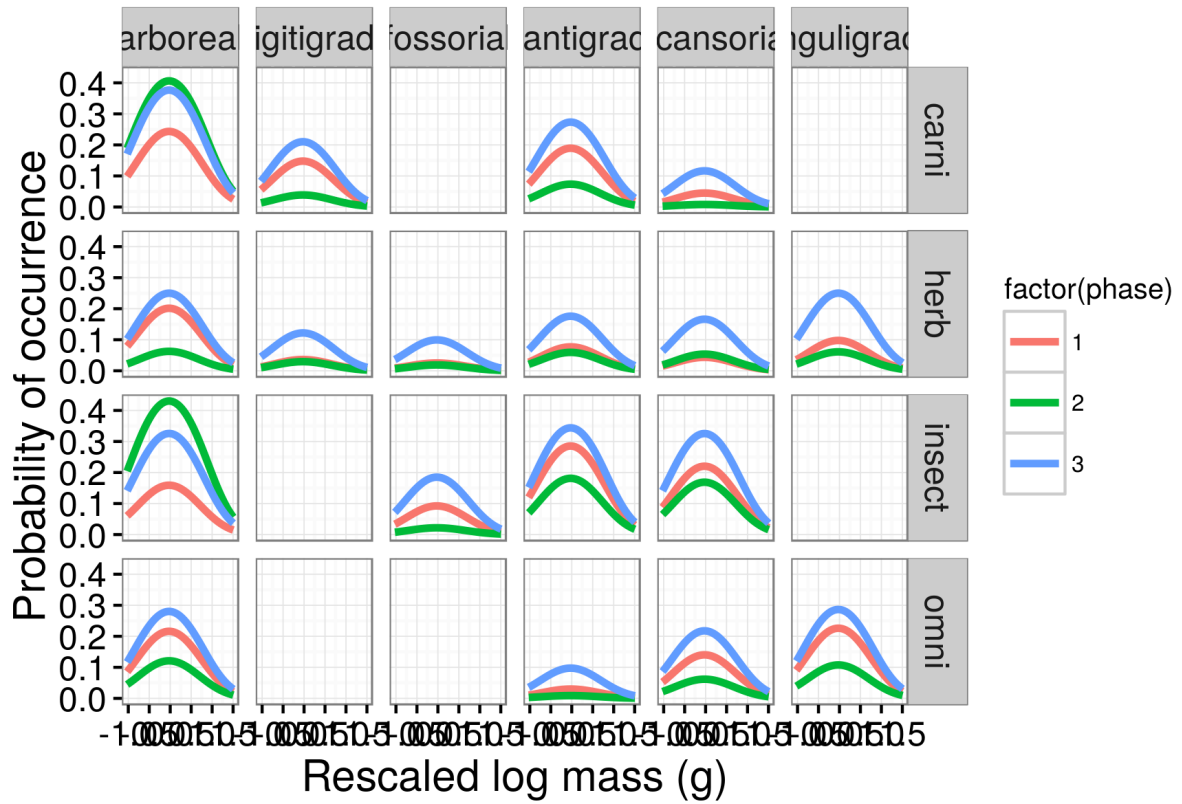


Figure 9: Mean estimate of the effect of species mass on the probability of a species originating for each of the three plant phases. The effect of mass is considered constant over time and that the only aspect of the model that changes with plant phase is the intercept of the relationship between mass and origination. The three plant phases are indicated by the color of the line. Mass has been log-transformed, centered, and rescaled; this means that a mass of 0 corresponds to the mean of log-mass of all observed species and that mass is in standard deviation units. Only the mean estimates of the effects of both mass and plant phase are plotted for clarity; these estimates are obviously made with uncertainty.

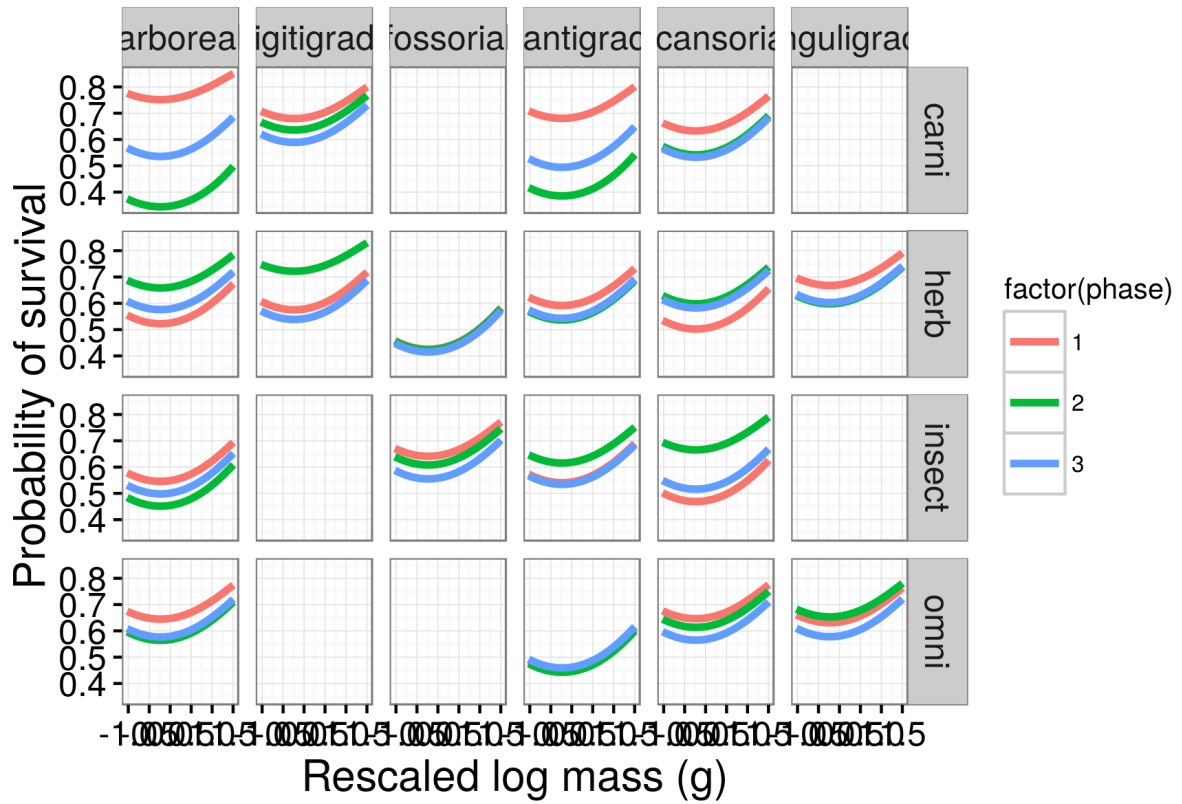


Figure 10: Mean estimate of the effect of species mass on the probability of a species survival for each of the three plant phases. The effect of mass is considered constant over time and that the only aspect of the model that changes with plant phase is the intercept of the relationship between mass and survival. The three plant phases are indicated by the color of the line. Mass has been log-transformed, centered, and rescaled; this means that a mass of 0 corresponds to the mean of log-mass of all observed species and that mass is in standard deviation units. Only the mean estimates of the effects of both mass and plant plant are plotted for clarity; these estimates are obviously made with uncertainty.

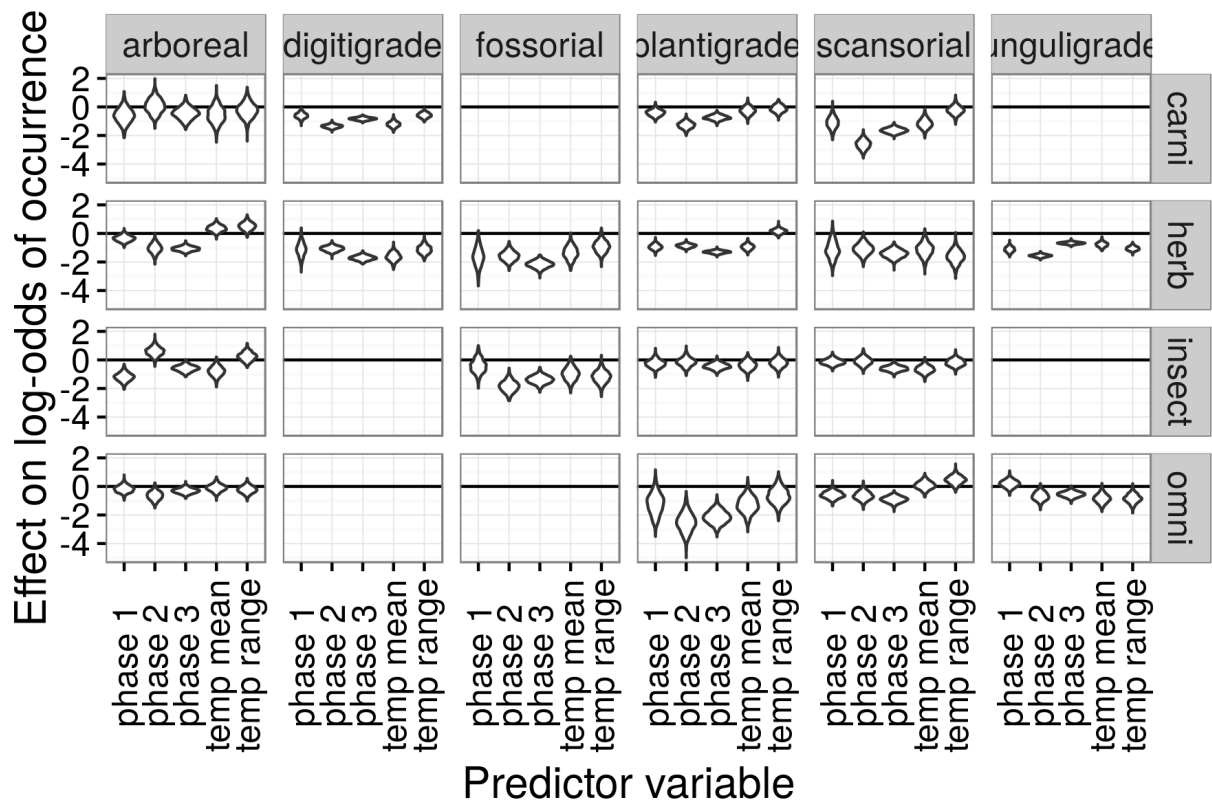


Figure 11: Estimated effects of the group-level covariates describing environmental context on log-odds of species occurrence. These estimates are from the pure-presence model.

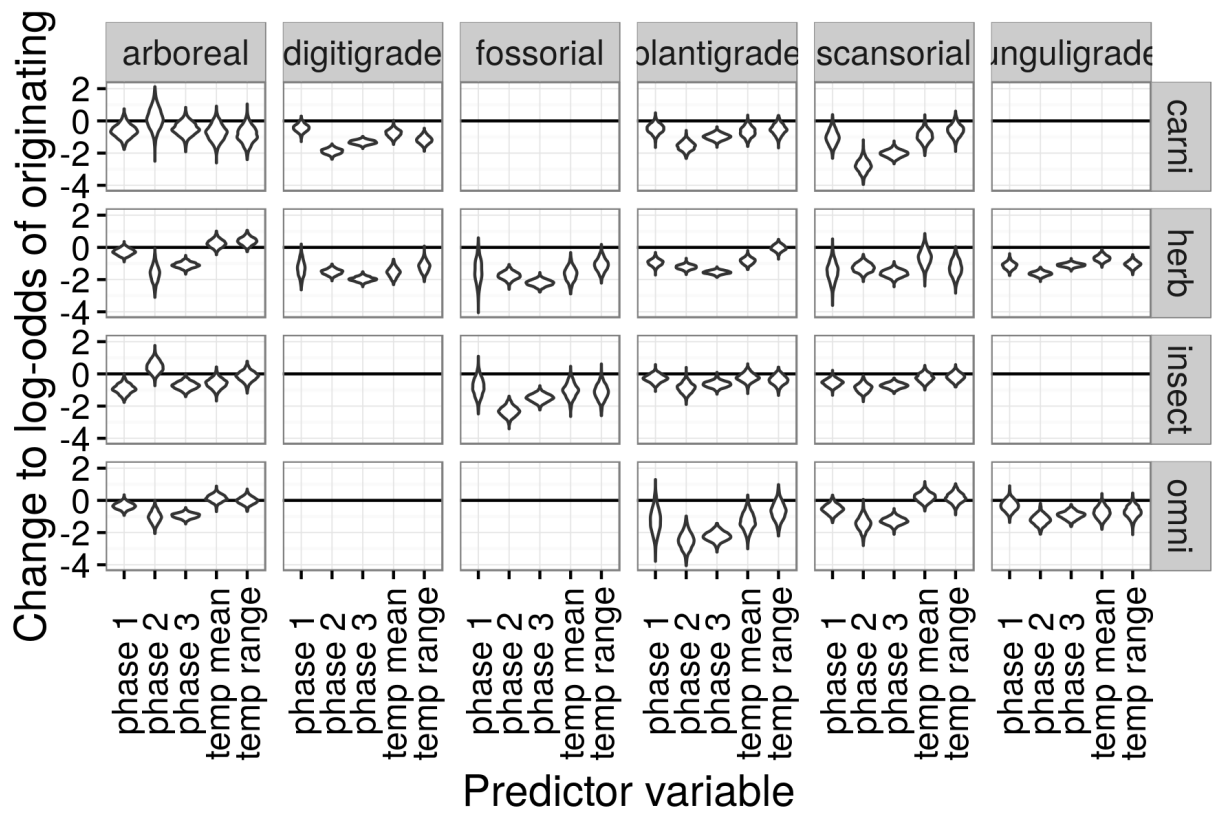


Figure 12: Estimated effects of the group-level covariates describing environmental context on log-odds of species origination. These estimates are from the birth-death model.

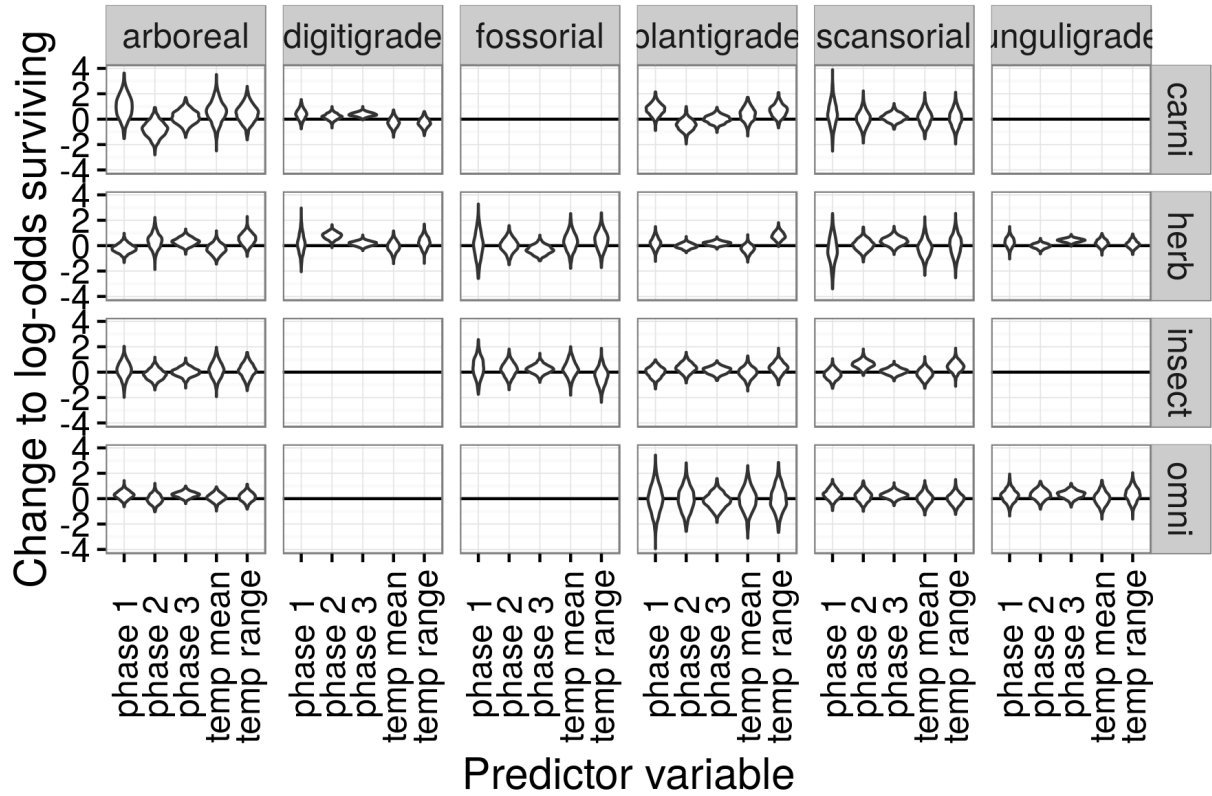


Figure 13: Estimated effects of the group-level covariates describing environmental context on log-odds of species survival. These estimates are from the birth-death model.

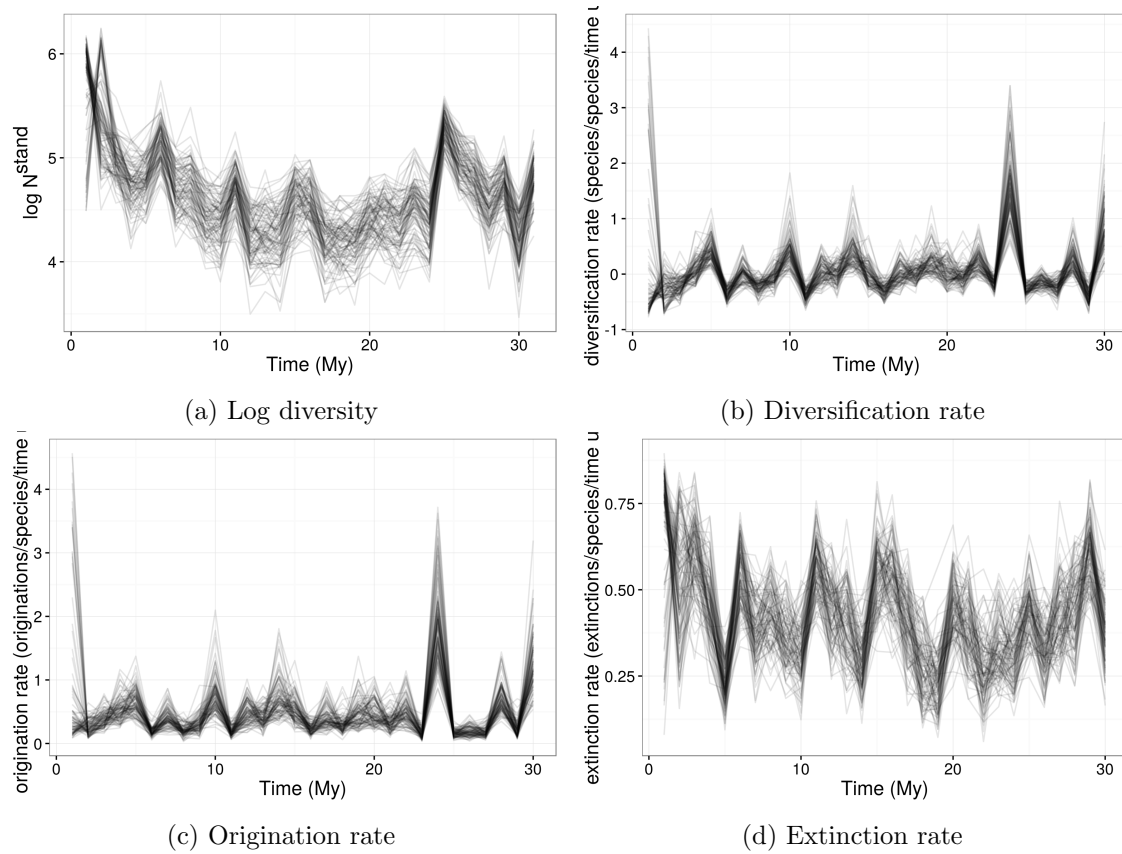


Figure 14: Posterior estimates of the time series of Cenozoic North American mammal diversity and its characteristic macroevolutionary rates; all estimates are from the birth-death model and 100 posterior draws are plotted to indicate the uncertainty in these estimates. The dramatic differences between diversity estimates at the first and second time points and the penultimate and last time points in this series are caused by well known edge effects in discrete-time birth-death models caused by $p_{-,t=1}$ and $p_{-,t=T}$ being partially unidentifiable (Royle and Dorazio, 2008); the hierarchical modeling strategy used here helps mitigate these effects but they are still present (Gelman et al., 2013; Royle and Dorazio, 2008). Diversification rate is in units of species gained per species present per time unit (2 My), origination rate is in units of species originating per species present per time unit, and extinction rate is in units of species becoming extinct per species present per time unit.

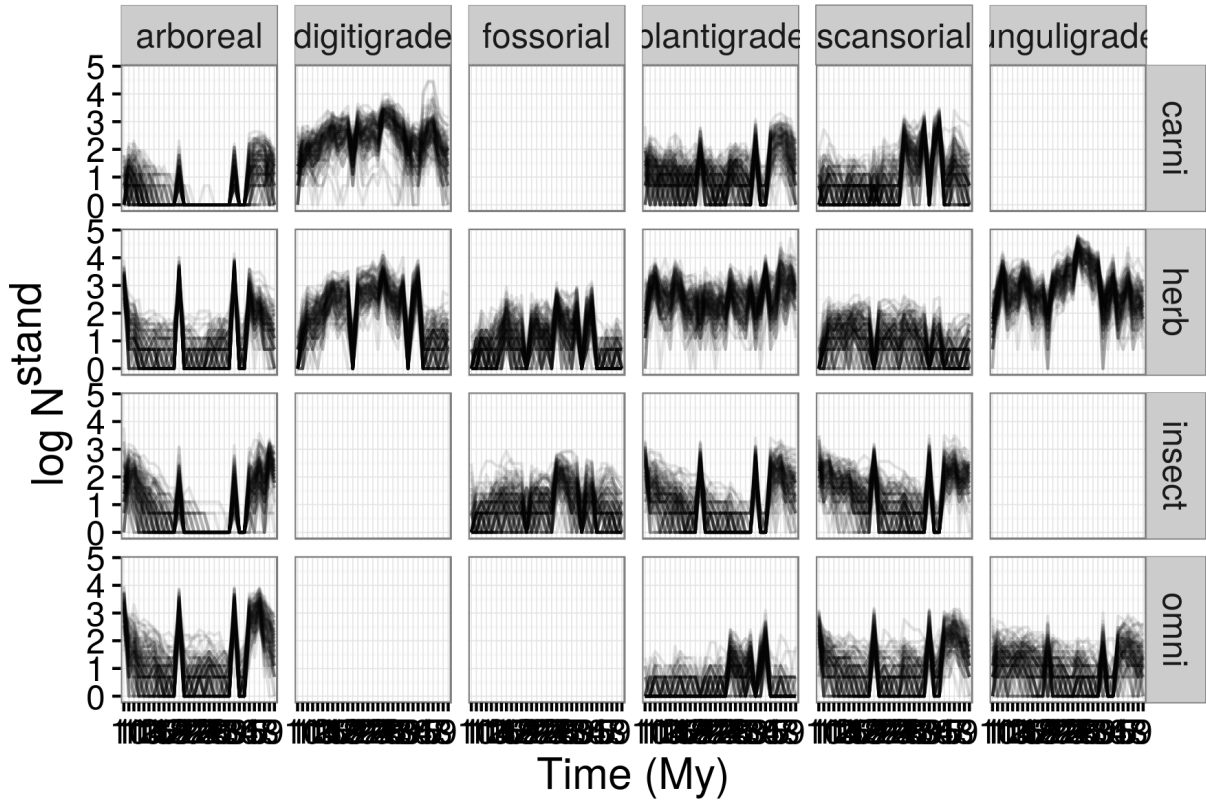


Figure 15: Posterior of standing log-diversity of North American mammals by ecotype for the Cenozoic as estimated from the birth-death model; 100 posterior draws are plotted to indicate the uncertainty in these estimates and what is technically plotted is log of diversity plus 1. The dramatic differences between diversity estimates at the first and second time points and the penultimate and last time points in this series are caused by well known edge effects in discrete-time birth-death models caused by $p_{-,t=1}$ and $p_{-,t=T}$ being partially unidentifiable (Royle and Dorazio, 2008); the hierarchical modeling strategy used here helps mitigate these effects but they are still present (Gelman et al., 2013; Royle and Dorazio, 2008).